ELSEVIER

Biophysical Chemistry 53 (1994) 57–68

Biophysical Chemistry

Protein and nucleic acid hydration and cosolvent interactions: Establishment of reliable baseline values at high cosolvent concentrations

Henryk Eisenberg [1]

Laboratory of Molecular Biology, NIDDK, National Institutes of Health, Building 5, Room 214, Bethesda MD 20892, USA

Received 15 February 1994; accepted 25 March 1994

Abstract

Hydration and cosolvent interactions of biological macromolecules can be derived, subject to excluded volume corrections, from studies of density increments at constant chemical potentials of diffusible solutes through a semipermeable membrane. In addition to precision density determinations of solutions dialyzed to equilibrium, the analytical ultracentrifuge, static and dynamic light and small angle X-ray and neutron scattering, and combined pairwise use of, for instance, ultracentrifugation and neutron scattering, considerably strengthen the experimental analysis and its interpretation. We have examined hydration of bovine serum albumin (BSA) in the native and denatured states, and binding of the denaturant guanidinium chloride (GdmCl) to the latter form; hydration of DNA and interaction with NaCl and CsCl; revised values of the halophilic malate dehydrogenase (hMDH) tetramer hydration and 'binding' of salts; probing of nucleosome core particle hydration as distinct from and additionally to the evaluation of volume exclusion (holes), by use of variously sized sugar related probes. Conclusions presented are compared to results from precision calorimetry and from X-ray crystallography structures, whenever applicable, and comparisons made with alternative interpretations and experimental approaches.

Keywords: Protein hydration; Nucleic acid hydration; Cosolvent interaction; Guanidinium chloride denaturation; Halophilic malate dehydrogenase

1. Introduction

Hydration of biological macromolecules is a highly important phenomenon as biological activity can only be generated if a minimum amount of water is provided [1]. When proteins or nucleic acids are hydrated the question arises whether hydration can basically be associated with the repeating units of the biological macromolecule, amino-acids or nucleotides, or whether hydration relates to a larger or smaller extent to the secondary, tertiary or quaternary structures of these macromolecules. We shall review in this work evidence [2–4] that hydration of proteins does not change extensively upon denaturation, and that therefore the major contribution to hydration may not be determined by the higher order structure of the native macromolecule (For an earlier review covering DNA hydration cf. Ref. [5]). Water molecules have, in recent years, been located in the interior and on the surface of the biological macromolecule by X-ray diffraction crystallography of proteins [6] and nucleic acids [7] in the crystalline state. A strongly emerging area of research

[1] Permanent address: Department of Structural Biology, Weizmann Institute of Science, Rehovot 76100, Israel.

SSDI 0301-4622(94)00076-V

reporting residence times of water molecules on protein surfaces is based on water-suppression NMR pulse sequences [8] and heteronuclear three-dimensional NMR [9]. Hydration can be defined in different ways which often carry an 'operational' connotation. The purpose of the present contribution is to dwell on difficulties, both with regard to concepts and to experiments, in our quest for a better understanding of a complex problem. We shall as well discuss the presence of additional components, cosolvents, stabilizing, maintaining, or destroying the biological native structure in solution.

Difficulties in determining hydration usually do not exist with respect to low molecular weight compounds. Magnesium chloride for instance may be dried to constant weight (at temperatures below its melting point, 714°C) or obtained in anhydrous crystalline form. The partial specific volume $\bar{v}$ (in ml/g) is defined in strict thermodynamic terms as the change in solution volume upon addition of one gram of dry solute to an adequate volume of water solvent to insure dilute solution conditions, at constant pressure P and temperature T. From the density ρ (in g/ml) determined at high accuracy, $\bar{v}$ is calculated by [10]

$$(\partial\rho/\partial c)_{P,T} = 1 - \bar{v}\rho^0, \qquad (1)$$

where c is the concentration in g/ml and ρ^0 is the density of the pure solvent. $MgCl_2$ is also available in crystalline form as a hexahydrate $MgCl_2.6H_2O$ (*bischofite*). The $\bar{v}$ of this entity (component) can be determined in similar fashion as above by dissolution and density determination. Hydration can be determined by quantitative loss of weight following drying of the hydrated crystals to constant weight above their melting (decomposition point), 116–118°C. Measurements of the partial specific volumes of the hydrated and non hydrated species and knowledge of the hydration number allows estimation of electrostriction (change in volume) of the water molecules upon hydration.

The procedure outlined above for low molecular weight compounds is not applicable to biological macromolecules, in particular proteins and nucleic acids with which our analysis is concerned. Thus double helical DNA denatures at uni/univalent salt concentrations below 1 mM, proteins and nucleic acids cannot usually be brought to complete dryness without irreversible loss of biological activity and the solution most likely, in addition to water (component 1) and macromolecule (component 2), also contains at least one additional cosolvent (component 3), be it an electroneutral salt or nonionic low molecular weight component. Hydration and cosolvent interactions must therefore be determined by measurements pertaining to the solution itself and not to the individual components. The saying "Water? That stuff around the battleships..." attributed to an Admiral of the Royal British Navy comes to mind. It is the purpose of this contribution to describe the baseline interactions of our macromolecular vessel of choice in a high sea of water at large concentrations of salts, non-ionic stabilizers or ionic denaturants. We shall not be concerned here with the unfolding process of proteins, for instance, but rather with the properties of native, on the one hand, and fully denatured protein molecules on the other. Much confusion is avoidable if it is recognized that the separate or combined use of various technologies in the study of hydration of macromolecules may lead to either identical, narrowly or widely differing results.

The classical concept of the hydrodynamic Stokes volume or radius [11,12] interprets flow and relaxation experiments, nowadays extended to electrophoretic gels, assuming idealized spherical or ellipsoidal impenetrable particles. This clearly is an unsatisfactory approach and translational and rotational diffusion constants of hydrated proteins have recently been simulated [13]. The use of thermodynamics in deriving a satisfactory measure of hydration and cosolvent interaction will be discussed in detail below. We shall see that 'thermodynamic' hydration correlates well with data obtained from X-ray crystallography, and therefore provides a good measure of protein and nucleic acid hydration and cosolvent interaction. Part of our discussion will be devoted to convincing the reader of this article that the term 'preferential' or 'selective' hydration or binding are confusing, have no defined physical content, do not lead to clarification of the subject under study and should therefore be avoided in further discussions.

The thermodynamic approach for the determination of solvent and cosolvent interaction parameters is based on the equilibrium dialysis experiment in which components diffusible through a semipermeable membrane reach constant chemical potentials μ [14,15]. The measurement of minute concentration differences across the semipermeable membrane was described for synthetic polyelectrolytes [16], yet hardly constitutes

a practical approach for high cosolvent concentrations. Density increments could be determined precisely with some effort by classical pycnometry [17] or with the then newly developed Kratky/Paar densitometer [18–21]. They critically depend on precise equilibration at high salt concentrations [22], whereas analytical equilibrium sedimentation, or velocity sedimentation and diffusion (from dynamic light scattering) provide these quantities more easily and with greater reliability if the molar mass M_2 is known [22]. If M_2 is known X-ray scattering is also useful for the determination of parameters relating to density increments [23], yet the method of choice is neutron scattering [24]. Novel information is obtained due to the negative neutron scattering density of H_2O, becoming positive with the use of D_2O. We shall in the following demonstrate advantages gained by the complementary use of ultracentrifugation, X-ray and neutron scattering.

2. Partial specific volumes of biological macromolecules

Biological macromolecules stable in pure water can be extensively dialyzed against water and their concentration determined by light absorption or by elemental analysis (nitrogen, phosphor, sulphur as the case may be), and translated into g/ml. As ρ usually varies linearly with c_2 at low values c_2, $\Delta\rho/c_2$ from a density measurement at a single concentration allows determination of $\bar{v}_2$ by Eq. (1). The partial special volumes $\bar{v}_2$ of proteins can be calculated to reasonable precision from the amino acid composition by summing the contributions of the amino acid residues as given by Cohn and Edsall [11], or from data in more recently critically discussed form [25].

The determination of $\bar{v}_2$ becomes more elaborate if the protein or nucleic acid is not stable in pure water. In that case and in the case when one wants to derive $\bar{v}_2$ at various salt or nonelectrolyte additive concentrations one may use the procedure described by Cohen and Eisenberg [17] for DNA solutions. The partial specific volume $\bar{v}_2$ is the change in volume per gram of component 2 added, at constant P, T and molality m_3 of component 3 (moles of component 3 per kg of component 1), or, more simply, the change in volume upon addition of component 2, at constant solute *composition*. The particle under investigation is dialyzed to equilibrium against low salt, in which it is stable. Concentration is determined optically as before, and the small concentration difference of component 3 across the dialysis membrane can be estimated, or neglected. Weighed amounts of component 3 are next added and dissolved and $(\partial\rho/\partial c_2)_{P,T,m_3}$ or, more simply, $(\Delta\rho/\partial c_2)_{P,T,m_3}$ determined by comparison with calibration solutions lacking component 2. The partial specific volume of DNA was found to depend on salt concentration [17,26] and is not merely the sum of purine and pyrimidine nucleotide components. This phenomenon relates to the high charge of the DNA double helix, as a similar dependence has not been observed in lower charge-density proteins in the native or denatured states [3,4,18].

3. Contrast variation of density increments at dialysis equilibrium

The density increment $(\partial\rho/\partial c_2)_\mu$ in multicomponent systems expresses, in distinction to the buoyancy relation (Eq. (1)), interaction with all other solvent components. Subscript μ signifies constancy of the chemical potential of all low-molecular weight components (the difference between $(\partial\rho/\partial c_2)_{T,\mu}$ and $(\partial\rho/\partial c_2)_{P,T,\mu_3}$, as determined in a dialysis equilibrium experiment is negligible and can be disregarded [10]). Restricting ourselves again for simplicity of expression to a three-component system, thermodynamic arguments at constant T, yield [10,15]

$$(\partial\rho/\partial c_2)_\mu = (1-\bar{v}_2\rho^0) + \xi_3(1-\bar{v}_3\rho^0) \quad (2a)$$

$$= (1+\xi_3) - \rho^0(\bar{v}_2+\xi_3\bar{v}_3), \quad (2b)$$

where the interaction parameter $\xi_3 = (\partial w_3/\partial w_2)_\mu$ represents the change in weight molality w_3 (g of component 3/g of component 1) with change in weight molality w_2 (g of component 2/g of component 1) required to maintain μ_1 and μ_3 constant. Eq. (2a) can be rewritten in totally symmetric fashion

$$(\partial\rho/\partial c_2)_\mu = (1-\bar{v}_2\rho^0) + \xi_1(1-\bar{v}_1\rho^0) \quad (3a)$$

$$= (1+\xi_1) - \rho^0(\bar{v}_2+\xi_1\bar{v}_1), \quad (3b)$$

and the interaction parameter ξ_1 is defined in analogous fashion to ξ_3. Each of these parameters represents interaction with both solvent and cosolvent components 1 and 3, and they are related by $\xi_1 = -\xi_3/w_3$ [10,27].

The relation of the interaction parameter ξ_3 to the partial derivatives μ_{23} and μ_{33} of the chemical potentials μ_2 and μ_3 with molality of component 3, at constant P, T and solution composition, is given [10,15] by

$$\xi_3 = (M_3/M_2)\mu_{23}/\mu_{33} + (M_3^2\bar{v}_3/\mu_{33})\, d\Pi/dw_2. \quad (4)$$

M_2 and M_3 are the molar masses (g/mol) of components 2 and 3 and Π is the osmotic pressure. The second term on the r.h.s. of Eq. (4) is negligible at low macromolecular concentrations. This establishes the connection with ligand theory considerations [28–30], with which we will not be concerned in this work.

The interaction parameter ξ_3 can, as mentioned, be determined directly by the measurement of minute concentration differences across a semipermeable membrane, at dialysis equilibrium. In a more reliable procedure $(\partial\rho/\partial c_2)_\mu$ is determined experimentally as already mentioned by accurate density determination of solutions in dialysis equilibrium, and ξ_3 or ξ_1 can then be calculated with the help of Eqs. (2) or (3), if the partial volumes are known at the given experimental conditions. This procedure involves the evaluation of small differences between large numbers. It has led to reliable results in the past [4,17,18], yet in one instance we have only recently [22] been able to obtain correct interaction parameters for halophilic malate dehydrogenase (hMDH) at very high concentrations of salt.

A powerful tool in the investigation of biological macromolecules is sedimentation in the analytical ultracentrifuge [31]. This method has now gained renewed increased attention [22,32] following the availability of a new generation of a state-of-the-art analytical ultracentrifuge (Optima XLA, Beckman). At high values of the angular velocity ω (sec^{-1}) solute particles sediment with a characteristic sedimentation velocity s (sec) as a result of the centrifugal field. The concentration gradients arising from the sedimentation process give rise to a diffusion field, and at suitably moderate centrifugation fields the sedimentation and diffusion processes balance and an equilibrium concentration gradient is established. The equilibrium sedimentation equation is derived from the basic thermodynamic requirement that, at sedimentation equilibrium, the chemical potentials μ of all the components in the ultracentrifuge tube be constant at all distances r from the center of rotation. This requirement, in the limiting case of low macromolecule concentration, leads to the following differential equation: [10,15,33]

$$d\ \ln c_2/dr^2 = (\omega^2/2RT)(\partial\rho/\partial c_2)_\mu M_2, \quad (5)$$

which can be easily integrated. At higher concentration the value of M_2 must be modified by virial corrections deriving from interactions between macromolecules [10,15,33]. Knowledge of $(\partial\rho/\partial c_2)_\mu$ allows precise determination of M_2 in the ultracentrifuge, yet no information concerning hydration or cosolvent interactions results from the above experiment. The value of M_2 may also be obtained from a combination of velocity sedimentation and the diffusion coefficient D, presently obtained by dynamic light scattering, by use of the classical Svedberg equation, extended to multicomponent systems [33]. In the limit of low macromolecular concentrations

$$RTs/D = (\partial\rho/\partial c_2)_\mu M_2 \quad (6)$$

In the time span in which I have been engaged in this research the emphasis and ultimate research objectives have undergone considerable change. Thus, three decades ago, it was highly important to obtain correct density and refractive index increments for the interpretation of sedimentation and light scattering experiments to enable the reliable determination of the molar mass and subunit structure of nucleic acids [34] and proteins such as the hexameric bovine liver glutamate dehydrogenase [35] or the establishment of the aldolase tetramer structure [18]. Now, more often than not, the peptide molar masses and amino acid sequences, as well as the subunit structures, are precisely known, culminating in the availability of high resolution X-ray diffraction structures. It thus becomes interesting to turn the carriage round, and to use the known values of the protein molar mass to calculate precise density increments and interaction parameters by use of analytical sedimentation and static and dynamic light scattering and, as will be discussed later, small angle X-ray and, in particular, small angle neutron scattering.

In most cases of experimental interest ξ_1 and ξ_3 are not constant with change in w_3, especially in the case of electrolyte cosolvents. We have observed a relationship of ξ_1 with w_3^{-1}, tending to linearity at high values of w_3 (Fig. 1) [3,4,22]. We observe relationships differing for different macromolecular solute systems, manifesting both positive and negative slopes, though

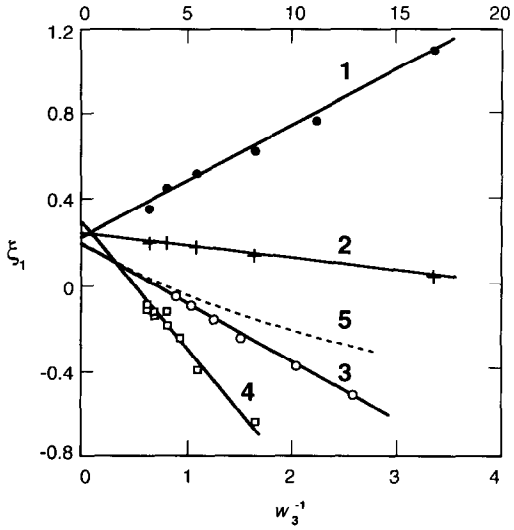

Fig. 1. Interaction parameter ξ_1, as a function of reciprocal cosolvent weight molality w_3^{-1} (g of water/g of cosolvent), for (1) DNA in NaCl, (2) BSA in NaCl, (3) BSA in GdmCl, (4) hMDH in NaCl, (5) BSA in GdmCl, curve calculated according to Ref. [43], cf. text, Section 6.1. Upper scale, NaCl, lower scale, GdmCl. Curves (1) to (3) from Ref. [3], data for curve (4) from Ref. [22].

the curves shown seem to aim at closely valued intercepts. We will provide a model, in Section 4, separating the interactions of component 2 with components 1 and 3, by analysis of these results. Parameters obtained from analytical sedimentation should be checked for pressure dependence in the range (up to about 100 atm) generated by the ultracentrifuge.

4. Model of solute/solvent/cosolvent interactions in multicomponent systems

We now describe a decomposition of the density increments which, for the first time in our discussion, leads towards an operational definition of hydration and solute/cosolvent interactions. The implications concerning $(\partial\rho/\partial c_2)_\mu$ when ξ_1 is linear with w_3^{-1}, as observed experimentally (Fig. 1) are as follows. We formally represent [24]

$$\xi_1 = p - q/w_3, \tag{7}$$

where p and q are constants, which for the moment have no model-related meaning. Using the relations [10]

$$c_1 + c_3 = \rho^0, \tag{8a}$$

$$c_1\bar{v}_1 + c_3\bar{v}_3 = 1, \tag{8b}$$

$$w_3 = c_3/c_1, \tag{8c}$$

valid at vanishing concentrations c_2, in Eqs. (3) and (7), we find

$$(\partial\rho/\partial c_2)_\mu = (1+p+q) - \rho^0(\bar{v}_2 + p\bar{v}_1 + q\bar{v}_3), \tag{9}$$

so that $(\partial\rho/\partial c_2)_\mu$ is linear with ρ^0 if $(\bar{v}_2 + p\bar{v}_1 + q\bar{v}_3)$ is constant. An invariant particle picture is next invoked [36], yielding a constant invariant volume $V_{tot} = (\bar{v}_2 + p\bar{v}_1 + q\bar{v}_3)$ per g of protein and a constant mass $(1+p+q)$ per gram of protein. The quantities p and q may be identified with associated water ($p = B_1$) and cosolvent ($q = B_3$) as defined by Reisler et al. [4]. When component 2 is highly charged as DNA, for instance, $q = B_3 - E_3 = B_3'$ where E_3 is a result of Donnan exclusion. The meaning of these quantities is that B_1 g of component 1 per g of component 2 and B_3' g of component 3 per g of component 2 are independently associated or 'bound' to component 2 and exclude the bulk solvent and cosolvent. We now write

$$(\partial\rho/\partial c_2)_\mu = (1 - \rho^0\bar{v}_2) + B_1(1 - \rho^0\bar{v}_1) + B_3'(1 - \rho^0\bar{v}_3), \tag{10a}$$

$$= (1 + B_1 + B_3') - \rho^0(\bar{v}_2 + B_1\bar{v}_1 + B_3'\bar{v}_3), \tag{10b}$$

which indicates that from the intercept and slope of the linear dependence of $(\partial\rho/\partial c_2)_\mu$ with ρ^0 it is possible to evaluate B_1 and B_3' if the partial specific volumes $\bar{v}_i$ are known and reasonably constant. The value of $V_{tot} = (\bar{v}_2 + B_1\bar{v}_1 + B_3'\bar{v}_3)$ can be cross-checked by the determination of the radius of gyration R_g from small angle X-ray [23] or neutron scattering [24] (Section 6.3) or by total volume calculation of data derived from X-ray crystallography [37,38] (Section 6.4). Caution should be exercised as we have already noted that $\bar{v}_2$ of DNA varies with salt concentration. We also emphasize that whereas the linear relationship in Eq. (10b) has meaningful significance for the evaluation of B_1 and B_3', the superficially similar Eqs. (2a) and (3a) can only be analyzed in similar fashion if ξ_3 and ξ_1 do not vary with cosolvent concentration. This is usually not the case. The linear dependence of $(\partial\rho/\partial c_2)_\mu$ with ρ^0 expresses the concept of the invariant particle hypothesis as stated by Tardieu et al. [36]. A more

complex situation, to be discussed in Section 6.1, would arise should B_1 or B_3' vary with solvent concentration.

We can now analyze the dependence of ξ_1 (or ξ_3) on cosolvent concentration by use of [4]

$$\xi_1 = B_1 - B_3'/w_3, \tag{11a}$$

or

$$\xi_3 = B_3' - B_1 w_3, \tag{11b}$$

which clearly indicate the dependence of ξ_1 or ξ_3 on both B_1 and B_3'. Only if B_3' equals zero or is close to it, can ξ_1 be identified with B_1, representing hydration; ξ_3 will always vary with w_3 for a hydrated macromolecule, whereas ξ_1 will be constant for vanishing B_3'.

The linear dependence of $(\partial\rho/\partial c_2)_\mu$ of halophilic malate dehydrogenase (hMDH), and bovine serum albumin (BSA), on ρ^0 in NaCl solutions is shown in Fig. 2 and will be discussed in Section 6, also in the context of X-ray and neutron scattering experiments. It is clear from the above presentation that the much emphasized term 'preferential' hydration or solvent or cosolvent interaction is not required for the physical interpretation of phenomena represented by a linear dependence of ξ_1 with w_3^{-1}, of ξ_3 with w_3 and of $(\partial\rho/\partial c_2)_\mu$ with ρ^0, above reasonably high cosolvent concentrations. 'Weak', in distinction to 'strong' interactions, have been extensively analyzed by Schellman [28–30] who proposes a model in which water of hydration exchanges with cosolvent at increasing cosolvent concentrations. This model is of great theoretical interest, yet it does not explain the limiting model at high cosolvent concentrations as discussed in this work. Timasheff [21] has recently proposed a

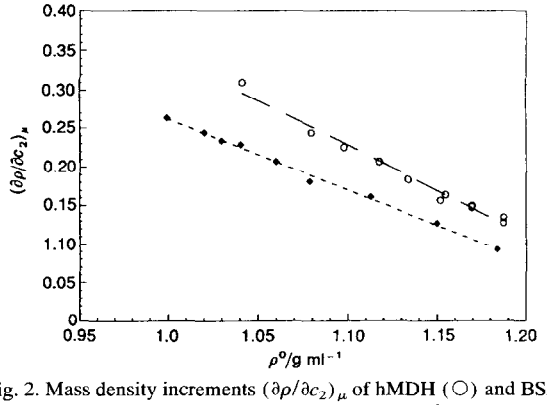

Fig. 2. Mass density increments $(\partial\rho/\partial c_2)_\mu$ of hMDH (○) and BSA (◆) in NaCl solutions as a function of mass density ρ^0 of the solvent. From Ref. [22], with permission.

detailed combined model containing both exchangeable and non-exchangeable solute/solvent and solute/cosolvent complexes, yet it seems experimentally difficult to distinguish between these groups. Studies ranging from very low to high cosolvent or denaturant concentrations in a protein unfolding process may require the application of more complex analysis, yet we see no alternative for the analysis in the limiting case of interest to us here. We shall analyze the results presented in Figs. 1 and 2 in Section 6 of this work.

5. Light, X-ray and neutron scattering

The light, $I(0)$, X-ray, $I_{el}(0)$ and neutron $I_N(0)$, forward-scattering intensities (calibrated by the scattering of standards of known scattering intensity under identical experimental conditions) are related to the refractive index, electron and neutron scattering density increments in the limiting case of low macromolecular concentrations (cf. Eq. (5)) by [27]

$$N_A I(0)/c_2 = (\partial n/\partial c_2)_\mu^2 M_2, \tag{12a}$$

$$N_A I_{el}(0)/c_2 = (\partial\rho_{el}/\partial c_2)_\mu^2 M_2, \tag{12b}$$

$$N_A I_N(0)/c_2 = (\partial\rho_N/\partial c_2)_\mu^2 M_2, \tag{12c}$$

where N_A is Avogadro's number. Similarly to the mass density increments (Eq. (3b)) the radiation scattering length density increments can be expressed as

$$(\partial\rho_{el}/\partial c_2)_\mu = l_2 + \xi_i l_i - \rho_{el}^0(\bar{v}_2 + \xi_i\bar{v}_i), \tag{13a}$$

$$(\partial\rho_N/\partial c_2)_\mu = b_2 + \xi_i b_i - \rho_N^0(\bar{v}_2 + \xi_i\bar{v}_i) \tag{13b}$$

where l_i and l_2 are electrons per g and b_i and b_2 (cm/g) the scattering lengths per g of water ($i=1$) or cosolvent ($i=3$) and protein (index=2) calculated from the chemical composition, respectively; ρ_{el}^0 (e cm^{-3}) is the electron density and ρ_N^0 (cm^{-2}) its neutron scattering density. The values of the l_i and b_i are listed in Table 1, from a study of halophilic malate dehydrogenase (Table 2, Ref. [24]). The important feature characterizing neutron scattering, or diffraction, is that, in distinction to the other parameters, b_1 is negative for water and changes sign when deuterium is substituted for hydrogen [39,40]. Light scattering and refractive index increments have been analyzed [22,41], but will not be discussed in this work. We can now express the equations for X-ray and neutron scattering in the for-

Table 1
Neutron scattering lengths, b_i, per gram [24] and l_i, electrons per gram [23], in water buffers in hMDH solutions, with permission

Neutrons (H_2O) (cm/g)	X-rays (e/g)
$b_1 = -5.62 \times 10^9$	$l_1 = 3.343 \times 10^{23}$
$b_2 = 14.8 \times 10^9$	$l_2 = 3.23 \times 10^{23}$
$b_3 = 13.59 \times 10^9$	$l_3 = 2.885 \times 10^{23}$

1 electron/gram is equivalent to 2.81×10^{-13} cm g^{-1}.

mulation corresponding to the mass density expression Eq. (10b).

$$(\partial\rho_{el}/\partial c_2)_\mu = (l_2 + B_1 l_1 + B_3' l_3) - \rho_{el}^0 V_{tot}, \quad (14a)$$

$$(\partial\rho_N/\partial c_2)_\mu = (b_2 + B_1 b_1 + B_3' b_3) - \rho_N^0 V_{tot}. \quad (14b)$$

If, as previously observed, the 'particle' volume is constant, as well as B_1 and B_3', then $(\partial\rho/\partial c_2)_\mu$, $(\partial\rho_{el}/\partial c_2)_\mu$ and $(\partial\rho_N/\partial c_2)_\mu$ versus ρ^0, ρ_{el}^0 and ρ_N^0, respectively, are straight lines with the same slope which is equal to the total volume of the particle, $V_{tot} = (\bar{v}_2 + B_1\bar{v}_1 + B_3'\bar{v}_3)$. It is thus possible to determine three parameters (B_1, B_3', $\bar{v}_2$) by solving Eqs. (10b) and (14b) or Eqs. (14a) and (14b), but a combination of Eqs. (10b) and (14a) is not useful in our work because of the similarity of the mass/electron ratios (cf. Table 1).

We have seen that mass density increments are obtained by direct density measurements, or from analytical ultracentrifugation (equilibrium or velocity sedimentation) in which the experimental parameter determined is $M_2\ (\partial\rho/\partial c_2)_\mu$. On the other hand radiation-scattering increments are determined from the forward-scattering intensity as $M_2\ (\partial\rho_{el}/\partial c_2)_\mu^2$ and $M_2\ (\partial\rho_N/\partial c_2)_\mu^2$.

We have proposed a new plot recently [22], which allows a joint analysis of all the scattering and mass

Table 2
Interaction parameters B_1 and $B_3' = B_3 - E_3$ of proteins and DNA in salt cosolvents, in units g water/g protein (DNA) and g cosolvent/g protein (DNA)

Substance	B_1	$B_3' = B_3 - E_3$
	g/g	
hMDH, NaCl	0.35–0.45	0.08–0.14
BSA, NaCl	0.23	0.012
BSA, GdmCl	0.18	0.27
DNA, NaCl	0.20	−0.054
DNA, CsCl	0.24	−0.070

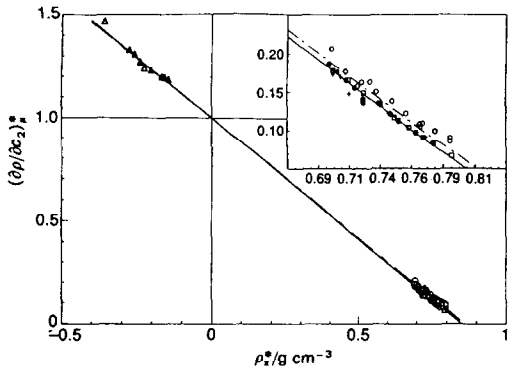

Fig. 3. $(\partial\rho/\partial c_2)_\mu^*$ versus ρ^{0*} (cf. Eq. (15)) for hMDH. In NaCl: (○), from densitometry; (□, +), from s/D; (×), from equilibrium sedimentation; (◇), from small angle X-ray scattering (SAXS), (△), from small angle neutron scattering (SANS); In KCl: (■), from equilibrium sedimentation; (●), from s/D; (▲), from SANS. The two close straight lines correspond to a total specific volume of 1.165 ml/g for NaCl and 1.178 ml/g for KCl. Insert, enlargement of the lower part of the plot (mass and SAXS data). From Ref. [22], with permission.

density increments. Eqs. (10b), (14a) and (14b) are each divided through by their respective intercept at zero solvent density (ρ^0, ρ_{el}^0 and ρ_N^0 equal to zero). The resulting 'reduced' density increments are dimensionless and can be plotted together as a function of solvent density also divided by the appropriate intercept. All points should now fall on the same straight line with an intercept of 1 and a slope of V_{tot} (Fig. 3),

$$\begin{aligned}(\partial\rho/\partial c_2)_\mu^* &= (\partial\rho_y/\partial c_2)_\mu/(x_2 + B_1 x_1 + B_3' x_3) \\ &= 1 - [\rho_y^0/(x_2 + B_1 x_1 + B_3' x_3)]\, V_{tot} \\ &= 1 - (\rho_y^0)^* V_{tot}, \end{aligned} \quad (15)$$

where subscript y is blank for mass, el and N for X-rays and neutrons, x_2 and x_i are unity for mass, l_2 and l_i for X-rays and b_2 and b_i for neutrons.

The complementarity between the neutron data, on one, and the X-ray and mass density, on the other hand, is clearly seen in Fig. 3. Neutron data, being close to null solvent scattering do not define a precise slope; they are, therefore not sensitive to the volume of the particle, but very sensitive to its composition through the value of the intercept $(b_2 + B_1 b_1 + B_3' b_3)$, which is well defined. On the other hand, the mass and X-ray values in our experiments are quite far from the intercept at zero solvent density, but they define the slope of the line and, therefore, are sensitive to the total volume of the particle.

6. Evaluation and analysis of selected experimental results

In Fig. 1 we have plotted ξ_1 (calculated by using Eq. (3a)) versus w_3^{-1} for a number of systems, which we interpret in terms of Eq. (11a). The intercept yields B_1 and the slope B_3'. The data are summarized in Table 2 and have mostly been analyzed before [3,4]. We note that the hydration values are rather similar for DNA, native proteins and denatured in guanidinium chloride (GdmCl), but the cosolvent interaction parameters B_3' differ strongly. Specific examples will now be discussed.

6.1. Bovine serum albumin

From Fig. 1 and Table 2 we see that BSA interacts weakly with NaCl, a phenomenon already observed by Scatchard et al. [14], but strongly with the denaturant GdmCl [4]. Recent results [22] ($B_1 = 0.187$ g/g and $B_3' \approx 0$ g/g, for NaCl) confirm the previous results and point to a level of reasonably accuracy. We can calculate hydration of the native protein based on a statistical analysis [42] of the atomic coordinates from 16 high-resolution X-ray diffraction data, used to study the distribution of water molecule sites around the 20 amino acid residues. From the BSA amino acid composition we calculate hydration equal to 0.234 g/g, in reasonable agreement with the value in Table 2. For GdmCl binding we find, from the slope and intercept in Fig. 1, $B_1 = 0.18$ g/g and $B_3' = 0.27$ g/g, which corresponds to 1.14 water and 0.32 GdmCl molecules per residue.

In a recent study of three native proteins and denatured in GdmCl and urea [43], precise calorimetric data were obtained by titrating native and denatured protein solutions with denaturants at various temperatures, and scanning them with temperature at various concentrations of denaturants. Consequently, in a number of steps the validity of which remains to be established, the authors suggest a procedure for deriving a binding model estimating the number of apparent binding sites of ribonuclease A, hen egg white lysozyme and cytochrome c, in the native and denatured forms. In the representation of identical noninteracting sites [12]

$$\bar{\upsilon} = nka_3/(1 + ka_3), \qquad (16)$$

where n is the total number of sites, $\bar{\upsilon}$ is the mean number of ligands bound, a_3 is the activity of component 3, and k is the intrinsic binding constant. Makhatadze and Privalov [43] determine from the calorimetric experiments average values at 25°C of $k = 0.6$ mol^{-1} for GdmCl and a considerably lower value 0.06 mol^{-1} for urea. They also obtain significantly more binding sites n for urea than for GdmCl. These conclusions therefore postulate variable cosolvent binding with varying cosolvent activity in contradiction to the invariant particle hypothesis at high cosolvent concentrations, which predicts a linear dependence of ξ_1 with w_3^{-1}.

We have calculated the expected variation of ξ_1 with w_3^{-1} for BSA in GdmCl, based on the Makhatadze and Privalov results. From $B_3' = 0.27$ g/g (Table 2) for BSA in GdmCl, which we identify with the limiting value n at infinite cosolvent concentration, we calculate $n = 187.5$ GdmCl per BSA molecules. With $k = 0.6$ mol^{-1} and published values of a_3 [43] we calculate by Eq. (16) values $B_3' = (M_3/M_2)\,\bar{\upsilon}$ as a function of w_3, from which we obtain ξ_1 by Eq. (11a) with $B_1 = 0.18$ (Table 2). The resulting upwards curving line is shown in Fig. 1. Following Makhatadze and Privalov, the binding constant of urea, which is one order of magnitude lower, should lead to considerably more curvature. To test the validity of the invariant particle hypothesis in comparison to a continuous cosolvent exchange and binding model at high cosolvent concentrations, and reach definitive conclusions for urea and GdmCl binding to denatured proteins, additional density increment measurements are required over a range of cosolvent concentrations.

In a recent work structural aspects of proteins unfolded in urea and in GdmCl have been explored [44].

6.2. Deoxyribonucleic acid

The slopes of the ξ_1 versus w_3^{-1} curves for DNA are positive (Fig. 1) in distinction to the protein curves, in which cosolvent 'binding' is involved; ξ_1 for DNA is always positive whereas for proteins with cosolvent 'binding' it is usually negative in the experimental range. Results for DNA in NaCl and in CsCl (not shown here) were reported by Cohen and Eisenberg [17] and later [4] analyzed in the present form. The

positive slope of the ξ_1 versus w_3^{-1} curves for highly charged DNA is due to exclusion of component 3 by the Donnan effect (see below). We have also more recently [26] summarized current aspects of DNA hydration including X-ray crystallography results on a B-DNA dodecamer [7]. We were pleased to observe the positive slope for the DNA curves, which strongly supported the model proposed and the analysis undertaken [4]: For this type of behavior we must have $E_3 > B_3$, that is, Donnan exclusion, E_3, must outweigh any binding B_3 of salt. If we again take that over the range examined ξ_1 varies linearly with w_3^{-1}, then we find for NaDNA in NaCl, B_1 equal to 0.20 g water/g of NaDNA and a minimum value E_3 (because of possible binding of salt B_3) equal to -0.054 g NaCl/g of NaDNA. In molar units this corresponds to 3.7 molecules of water bound and 0.3 molecules of NaCl excluded per phosphate or base (of average molecular weight 331). These numbers are very reasonable, both in terms of the water molecules, which can be accommodated in the wide and narrow grooves of double helical DNA, and the Donnan exclusion, which can be estimated [45] from the solution of the Poisson–Boltzmann equation for rod-like particles. For CsDNA in CsCl we find $B_1 = 0.24$ g water/g of CsDNA and $E_3 - B_3 \approx 0.07$ g of CsCl/g of CsDNA or, in molar terms, 5.9 molecules of water bound and 0.19 molecules of CsCl excluded per molecule of phosphate or base (of average molecular weight 441). On the average we therefore found 4.8 or ≈ 5 molecules of water per nucleotide, with an uncertainty of one.

A current theoretical analysis of effects on DNA/ligand binding compares Poisson–Boltzman and counterion binding/release models [46].

In subsequent X-ray crystallographic studies [7] it was found that the ordered water structure around a B-form dodecamer consists of an average of 3 water molecules per backbone phosphate group and 2 from the grooves (one each from the major and minor grooves), a total of 5 water molecules, with an uncertainty of one. This result compares well with the value previously determined by us from thermodynamic volume considerations. Thus, water molecules which are 'localized' in the X-ray crystallographic sense, appear similar in considerations relating to volume exclusion in a thermodynamic sense. These numbers are much lower than what had been earlier estimated [5,26] to constitute the primary hydration shell of DNA impermeable to ions, to comprise about 20 water molecules per nucleotide. The X-ray investigations were more recently extended on B-form decamers to higher resolution [47] and the influence of the environment on A, B and Z DNA structures determined by X-ray crystallography has been analyzed [48,49].

It is interesting to note that a recent review providing a wealth of historical and recent references on DNA hydration [50] reports "there are at least two hydration layers: the first consisting of approximately 20 water molecules per nucleotide is impermeable to ions."

6.3. *Halophilic malate dehydrogenase*

The data referring to hMDH in Fig. 1 and Table 2 are different from the data we have previously published [51]. Recently we have isolated the hMDH gene, expressed it in *E. coli*, and sequenced the protein peptide subunit [52]. Its molar mass was found to be 32638 g/mol, significantly smaller than the value previously accepted [41]. The density increments reported before were redetermined with great care [22], and we could show that hMDH is a tetramer, homologous and similar to tetrameric lactate dehydrogenase, rather than a dimer, as most malate dehydrogenases are. As already mentioned earlier, the determination of ξ_1 from Eq. (3a) is a difficult process, true dialysis equilibrium conditions must be achieved to determine small density differences and partial specific volumes must be known for the evaluation. The hMDH system is particularly difficult to analyze pre-

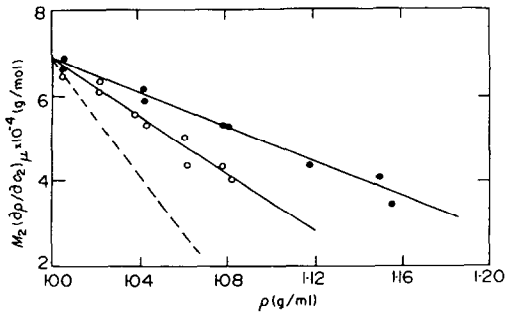

Fig. 4. The slopes $M_2 (\partial\rho/\partial c_2)_\mu$ for nucleosome core particles, from equilibrium sedimentation against solvent mass-density ρ^0. Density contrast variation solutes: (●), sucrose ($\xi_1 = 0.318$); (○), γ-cyclodextrin ($\xi_1 = 1.005$). Broken curve is the dextran curve ($\xi_1 = 2.32$) from Fig. 14 of Ref. [37]. From Ref. [38], with permission.

cisely at high salt concentrations. We shall see below (Figs. 2–4) that linear plots of the density increments vs. the solvent density are a good way to derive B_1 and B_3', combining mass or X-ray with neutron scattering data [22]. However the data obtained by both technologies are now in reasonable agreement. We have thus established that hMDH hydration is only slightly higher than that of other non-halophilic proteins, yet NaCl 'binding' is much in excess of that of non-halophilic proteins.

In Fig. 2 we plot $(\partial\rho/\partial c_2)_\mu$ versus ρ^0 for hMDH and BSA [22]. A complete analysis of the hMDH data by mass, X-ray and neutron scattering is given in Fig. 3 where $(\partial\rho/\partial c_2)^*_\mu$ is plotted versus $(\rho^0_x)^*$ (Eq. (15)). The complementarity of the data, as discussed in Section 5, is clearly seen here, and values for $B_1 = 0.35$–0.45, $B_3' = 0.08$–0.14 g/g and $\bar{v}_2 = 0.73$ ml/g have been obtained [22]. We estimate from X-ray crystal structure analysis of a range of proteins [42] a hydration of 0.252 g water/g hMDH based on its amino acid composition, which is lower than the experimental average $B_1 \approx 0.40$ g/g. This may be due to the halophilic nature of the protein or to its being a tetramer, with spaces excluded not available to the salt cosolvent. For the total volume V_{tot} (Eq. (10b) we calculate 253.7 nm^3/molecule, which corresponds satisfactorily to 268 nm^3/molecule, calculated, at this stage, for a spherically shaped hMDH tetramer with a radius of gyration $R_g = 3.1$ nm, averaged from the experimental data [24]. hMDH at high salt concentrations is one of the most difficult systems for study we have encountered. The role of the salt interactions is assuming increasing relevance in this system and is currently being determined on a molecular level by a high-resolution X-ray crystal diffraction study recently completed (O. Butbul-Dym and J. Sussman, in preparation) which, we believe, will answer many of the questions that have been raised. The study of hMDH is of great interest and significance in trying to understand adaptation to extreme biological environments. A neutron scattering study of hMDH in D_2O has been completed (F. Bonnete and G. Zaccai, J. Mol. Biol., in press). The authors conclude that the stability of hMDH is significantly higher in D_2O than in H_2O, the protein is stable at relatively low salt concentrations, yet both V_{tot} and the solvent/cosolvent interactions are similar and the stabilization model previously proposed [53] applies in both D_2O and H_2O.

6.4. Nucleosome core particles

In another set of experiments we have determined the linear variation of $(\partial\rho/\partial c_2)_\mu$ versus ρ^0, of solutions of nucleosome core particles [37,38], fractally probing with small sugars (sucrose, raffinose, glycerol) which are believed not to interact but penetrate into the core particle and determine hydration, and large sugars such as dextran and cyclodextrin (Fig. 4), which do not penetrate into the core particle and therefore determine the total volume, composed of excluded and basic chemical volume. The large dextran probe yields exclusion volumes which are too large (Fig. 4), due to the excessive size of the probe.

In these experiments $B_3' \approx 0$ and therefore $\xi_1 = B_1$. For sucrose (upper curve Fig. 4) we [38] calculate $B_1 = 0.318$ g/g and $\bar{v}_2 = 0.662$ ml/g, which agrees with the earlier result [37]. From the value of B_1 we calculate a volume of hydration of 108 nm^3 per nucleosome core particle. The middle curve in Fig. 4 yields an identical value for $\bar{v}_2 = 0.665$ ml/g and $B_1 = 1.005$ g/g from contrast variation with γ-cyclodextrin. This corresponds to 341 nm^3 per nucleosome core particle. The total volume V_{tot} of the nucleosome core particle equals $(\bar{v}_2 + B_1\bar{v}_1)(M_2/N_A) = 561$ nm^3, which agrees with scattering and hydrodynamic data (542 nm^3) [37] and with the X-ray crystallographic results [54], allowing for the existence of considerable holes in the nucleosome core particle. Sucrose or glycerol, which should be capable of penetrating holes larger than ≈ 0.3 nm, have access to all spaces inside the core particle and probe for hydration spaces. On the other hand, γ-cyclodextrin, which is a toroidal molecule with a major cross section of about 1.6 nm, demonstrates zero penetration into the core particle. Thus, whatever the geometry of the core particle in solution, the diameter of the holes on the surface of the particle, must be smaller than 1.6 nm and larger than 0.3 nm.

In our studies with sugars as cosolvents we usually found $B_3' \approx 0$, and therefore ξ_1 is independent of cosolvent concentration when the cosolvent does not interact with component 2. This was also found in protein/sucrose studies [55,56]. It must, in all cases, be established with care if the cosolvent does indeed not interact with component 2, and experiments must be performed and reported over a range of cosolvent concentrations. In the case of chromatin, for instance, glycerol interacts with component 2, whereas most sugars do not (Ghir-

lando et al. unpublished). Recently it was shown [57] that sucrose and other hydroxylic compounds affect the salt-induced B-to-Z transition of poly [d(G–C)], providing evidence for the thermodynamic role of water activity beyond the invariant particle conditions, discussed in our work. Another important aspect of the problem, still requiring extensive investigation (Ghirlando et al. unpublished), concerns the role of excluded volume [58] when noninteracting cosolvents of variable size are used in these studies of fractal probing. Such studies may lead to modifications of parameters previously calculated. Excluded volume corrections may be more significant when probing with bulky organic molecules than with more compact inorganic salts.

7. Conclusions

We believe to have shown that problems of hydration and cosolvent interactions at high cosolvent concentrations in solutions of biological macromolecules can be analyzed by a straightforward thermodynamic approach and that a significant part of water believed to constitute 'hydration' is strongly associated with the biopolymer subunits. This concept has been advanced at an early stage of the game [2] yet we believe that the thermodynamic approach, though leading to values subject to reasonable experimental uncertainties, represents a reliable way of evaluating hydration in a solute medium. The thermodynamic approach in addition presents a valid representation of the more complex systems, including cosolvents, major components of the biological system, though we have limited our discussion for practical reasons to a single cosolvent, of ionic or non-ionic type, in each experimental system. An added advantage of the thermodynamic investigation is that its performance proceeds at low concentrations of component 2 in natural media, which can be widely varied, and that abnormal conditions such as freezing or addition of organic components, which may affect the phenomena under investigation, is not required. We have also been able to show that by varying the cosolvent size it is possible to fractally probe variously sized domains of exclusion which, on top of the spaces excluded by hydration, are not accessible to the variably sized probes.

We cannot conclude this work on nucleic acid and protein hydration and cosolvent interactions at high cosolvent concentrations, without taking again notice that powerful methodologies such as X-ray and neutron diffraction [59], and nuclear magnetic resonance [60–62], have now become available for the determination of hydration of biological macromolecules in the crystalline state or in concentrated solutions. In a recent review [63] both the virtues and the problematics of X-ray crystallography, NMR and model simulations for the determination of protein hydration are clearly presented. As indicated in the title of this work, we consider the results obtained by us for a number of systems to constitute baseline values at high cosolvent concentrations. The thermodynamic results represent long-time averaged equilibrium values, in distinction to the time resolved NMR studies. The true power of science resides in the ability to successfully combine results from complementary methodologies to cover a variety of aspects and conditions characterizing complex biological systems. I have aimed to show in this analysis that the study of solution properties of biological macromolecules is still justified in this age of experimental sophistication.

Acknowledgements

I would like to thank colleagues, co-workers and friends who have contributed and critically analyzed the contents of this work.

References

[1] R.B. Gregory, M. Gaugoda, R.K. Gilpin and W. Su, Biopolymers 33 (1993) 1871–1876.
[2] I.D. Kuntz, J. Am. Chem. Soc. 93 (1971) 514–516.
[3] H. Eisenberg, Y. Haik, J.B. Ifft, W. Leicht, M. Mevarech and S. Pundak, in: Energetics and structure of halophilic microorganisms, eds. S.R. Kaplan and M. Ginzburg (Elsevier, Amsterdam, 1978) pp. 13–32.
[4] E. Reisler, Y. Haik and H. Eisenberg, Biochemistry 16 (1977) 197–203.
[5] H. Eisenberg, in: Basic principles in nucleic acids, Vol. 2, ed. P.O.P. Ts'o (Academic Press, New York, 1974) pp. 171–264.
[6] A. Wlodawer, J. Nachman, G.L. Gilligand, W. Gallagher and C. Woodward, J. Mol. Biol. 198 (1987) 469–480.
[7] M.L. Kopka, A.V. Fratini, H.R. Drew and R.E. Dickerson, J. Mol. Biol. 163 (1983) 129–146.

[8] G. Otting, E. Liepinsh and K. Wutrich, Science 254 (1991) 974–980.
[9] G.M. Clore and A.M. Gronenborn, J. Mol. Biol. 223 (1992) 853–856.
[10] H. Eisenberg, Biological macromolecules and polyelectrolytes in solution (Clarendon Press, Oxford, 1976).
[11] E.J. Cohn and J.T. Edsall, Proteins, amino acids and peptides (Reinhold, New York, 1943).
[12] C. Tanford, Physical chemistry of macromolecules (Wiley, New York, 1961).
[13] P.E. Smith and W.F. van Gunsteren, J. Mol. Biol. 236 (1994) 629–636.
[14] G. Scatchard, A.C. Batchelder and A. Brown, J. Am. Chem. Soc. 68 (1946) 2320–2329.
[15] E.F. Casassa and H. Eisenberg, Advan. Prot. Chem. 19 (1964) 287–395.
[16] U.P. Strauss and P. Ander, J. Am. Chem. Soc. 80 (1958) 6494–6498.
[17] G. Cohen and H. Eisenberg, Biopolymers 6 (1968) 1077–1100.
[18] E. Reisler and H. Eisenberg, Biochemistry 8 (1969) 4572–4578.
[19] J.C. Lee and S.N. Timasheff, Biochemistry 13 (1974) 257–265.
[20] J.C. Lee, K. Gekko and S.N. Timasheff, Methods Enzym. 61 (1979) 26–57.
[21] S.N. Timasheff, Ann. Rev. Biophys. Biomol. Struct. 22 (1993) 63–97.
[22] F. Bonnété, C. Ebel, G. Zaccai and H. Eisenberg, J. Chem. Soc. Faraday Trans. 89 (1993) 2659–2666.
[23] M.H. Reich, Z. Kam and H. Eisenberg, Biochemistry 21 (1982) 5189–5195.
[24] G. Zaccai, E. Wachtel and H. Eisenberg, J. Mol. Biol. 190 (1986) 97–106.
[25] S.J. Perkins, Eur. J. Biochem. 157 (1986) 169–180.
[26] H. Eisenberg, in: Landolt-Bornstein New Series Biophysics – Nucleic Acids, Vol 7/1c, ed. W. Saenger (Springer, Berlin, 1990) 257–276.
[27] H. Eisenberg, Quart. Rev. Biophys. 14 (1981) 142–172.
[28] J.A. Schellman, Biopolymers 26 (1987) 549–559.
[29] J.A. Schellman, Biophys. Chem. 37 (1990) 121–140.
[30] J.A. Schellman, Biophys. Chem. 45 (1993) 273–279.
[31] K.E. van Holde, in: The Proteins, 3rd Ed. Vol. 2, eds. H. Neurath and R.L. Hill (Academic Press, New York, 1975) pp. 225–291.
[32] D.J. Clark, R. Ghirlando, G. Felsenfeld and H. Eisenberg, J. Mol. Biol. 234 (1993) 297–301.
[33] H. Eisenberg, J. Chem. Phys. 36 (1962) 1837–1843.
[34] G. Voordouw, Z. Kam, N. Borochov and H. Eisenberg, Biophys. Chem. 8 (1978) 171–189.
[35] H. Eisenberg and G.M. Tomkins, J. Mol. Biol. 31 (1968) 37–49.
[36] A. Tardieu, P. Vachette, A. Gulik and M. Le Maire, Biochemistry 20 (1981) 4399–4406.
[37] H. Eisenberg and G. Felsenfeld, J. Mol. Biol. 150 (1981) 537–555.
[38] K.O. Greulich, J. Ausio and H. Eisenberg, J. Mol. Biol. 186 (1985) 167–173.
[39] B. Jacrot and G. Zaccai, Biopolymers 20 (1981) 2413–2426.
[40] G. Zaccai and B. Jacrot, Ann. Rev. Biophys. Bioeng. 12 (1983) 139–157.
[41] H. Eisenberg, Biochem. Soc. Symp. 58 (1992) 113–125.
[42] N. Thanki, J.M. Thornton and J.M. Goodfellow, J. Mol. Biol. 202 (1988) 637–657.
[43] G.I. Makhatadze and P.L. Privalov, J. Mol. Biol. 226 (1992) 491–505.
[44] T.M. Logan, Y. Thériault and S.W. Fesik, J. Mol. Biol. 236 (1994) 637–648.
[45] L.M. Gross and U.P. Strauss, in: Chemical physics of ionic solutions, eds. B.E. Conway and R.G. Barradas (Wiley, New York, 1966) pp. 361–389.
[46] K.A. Sharp, V. Misra, R. Friedman, J. Hecht and B. Honig, Biophys. J. 66 (1994) A291.
[47] G.G. Privé, K. Yanagi and R.E. Dickerson, J. Mol. Biol. 217 (1991) 177–180.
[48] Z. Shakked, G. Guerstein-Guzikevich, M. Eisenstein, F. Frolow and D. Rabinovich, Nature 342 (1989) 456–460.
[49] Z. Shakked, Curr. Opin. Struct. Biol. 1 (1991) 446–451.
[50] H.M. Berman, Curr. Opin. Struct. Biol. 1 (1991) 423–427.
[51] H. Eisenberg, M. Mevarech and G. Zaccai, Advan. Protein Chem. 43 (1992) 1–62.
[52] F. Cendrin, J. Chroboczek, G. Zaccai, H. Eisenberg and M. Mevarech, Biochemistry 32 (1993) 4308–4313.
[53] G. Zaccai and H. Eisenberg, Trends. Biochem. Sci. 15 (1990) 333–337.
[54] T.J. Richmond, J.T. Finch, B. Rushton, D. Rhodes and A. Klug, Nature 311 (1984) 532–537.
[55] J.C. Lee and S.N. Timasheff, J. Biol. Chem. 256 (1981) 7193–7201.
[56] H.B. Bull, Arch. Biochem. Biophys. 208 (1981) 229–232.
[57] Y. Choe, B.J. Short Jr., H.H. Chen, R.S. Preisler and D.C. Rau, Biophys. J. 66 (1994) A158.
[58] T. Arakawa and S.N. Timasheff, Biochemistry 24 (1985) 6756–6762.
[59] J.S. Finer-Moore, A.A. Kossiakoff, J.W. Hurley, T. Earnest and R.M. Stroud, Proteins 12 (1992) 203–222.
[60] M.G. Kubinec and D.E. Wemmer, Curr. Opin. Struct. Biol. 2 (1992) 828–831.
[61] K. Wüthrich, G. Otting and E. Liepinsk, Faraday Discuss. 93 (1992) 35–45.
[62] G.M. Clore, A. Bax, J.G. Omichinski and A.M. Gronenborn, Structure 2 (1994) 89–94.
[63] M. Levitt and B.H. Park, Structure 1 (1993) 223–226.